JOWRM

Journal of Water Resources Management

Journal homepage: https://journal.water.gov.my

e-ISSN: 2811-3578

Experimental Investigation of Hydraulic Resistance Behaviour in Subsurface Drains under Downstream Backflow Conditions

Junaidah Abdullah [1,a], Mohd Remy Rozainy Mohd Arif Zainol [1,2,b*], Mohd Sharizal Abdul Aziz[3,c] , Chong Khai Lin [4,d], Noor Aida Saad [1,e], Chang Chun Kiat [1,f], Khairul Rahmah Ayub [1,g], Syafiq Shaharuddin[1,h]

[1] River Engineering and Urban Drainage Research Centre (REDAC), Tuanku Syed Sirajuddin Engineering Campus, Universiti Sains Malaysia, 14300 Nibong Tebal Penang, MALAYSIA

[2] School of Civil Engineering, Tuanku Syed Sirajuddin Engineering Campus, Universiti Sains Malaysia 14300 Nibong Tebal Penang, MALAYSIA

[3] School of Mechanical Engineering, Tuanku Syed Sirajuddin Engineering Campus, Universiti Sains Malaysia 14300 Nibong Tebal Penang, MALAYSIA

[4] Disaster Management Institute School of Technology Management and Logistics Universiti Utara Malaysia, 06010 Sintok Kedah, MALAYSIA

Email: [a]junaidahabdullah@usm.my, [b]ceremy@usm.my, [c]msharizal@usm.my, [d]klchong@uum.edu.my, [e]aidasaad@usm.my [f]redac10@usm.my, [g]redac03@usm.my, [h]redacsyafiq@usm.my

Received 26 Feb 2026;
Accepted 29 Jun 2026;
Available online 30 Jun 2026

Abstract: Urban flash floods can induce downstream backflow conditions that significantly alter the hydraulic behaviour of subsurface drainage systems. Although perforated and modular subsurface drains are widely used in stormwater management, their hydraulic resistance characteristics under restricted outlet conditions remain insufficiently understood. This study experimentally investigates the flow behaviour of perforated subsurface drains (PSD) and subsurface drain modules (SDM) under controlled backflow conditions induced by a partially open gate at a constant water depth of 10 cm. Experiments were conducted in a laboratory flume at three longitudinal slopes (1:500, 1:750, and 1:1000) to assess slope-dependent responses. The relationships between Manning's roughness coefficient (*n*), velocity (*V*), flow depth (*y*), and Froude number (*Fr*) were analysed. At 1:500, stable inverse n–v relationships were observed, whereas correlation strength deteriorated markedly at 1:1000, indicating increasing boundary-controlled backwater influence. Weak linear associations between n and flow depth suggest that effective roughness under partial submergence cannot be described solely by depth variation. The n–Fr relationship further demonstrated regime-dependent resistance behaviour, particularly under mild gradients. SDM exhibited comparatively more stable resistance characteristics across slopes, while PSD showed greater turbulence sensitivity under partially submerged conditions. These findings highlight the necessity of incorporating downstream boundary effects in the design of resilient urban subsurface drainage systems.

Keywords: Downstream backflow, Hydraulic resistance, Subsurface drainage systems

1. Introduction

Flooding remains one of the most destructive natural hazards affecting infrastructure, economic stability, and human safety worldwide. In urban environments, the proliferation of impervious surfaces such as roads, pavements, and buildings significantly alters the natural hydrological cycle by reducing infiltration capacity and accelerating surface runoff (Si et al., 2023). As a result, stormwater is rapidly conveyed into drainage networks, frequently exceeding their design capacity and increasing the likelihood of urban inundation even during moderate rainfall events. The situation is exacerbated when drainage systems are inadequately designed, poorly maintained, or incapable of accommodating extreme hydrological variability.

Flash floods are particularly hazardous due to their rapid onset and high flow velocities. Peak discharge may occur within hours of intense rainfall, leaving minimal time for mitigation (Dordevic et al., 2020) Globally, floods account for nearly half of all weather-related disasters and represent a significant proportion of disaster-induced fatalities and economic losses. In urban catchments, intense convective storms or monsoonal rainfall frequently overwhelm

**Corresponding author: ceremy@usm.my*
2024 JPS Publishing. All right reserved.

stormwater infrastructure when runoff generation exceeds drainage capacity (Hammond et al., 2015) Beyond inundation depth, the destructive capacity of flash floods arises from high flow energy, debris transport, and the consequent structural and socio-economic disruption (Maqtan et al., 2022)

In Malaysia, flash floods have become increasingly frequent in both urban and peri-urban regions, representing the most recurrent natural hazard nationwide (Maqtan et al., 2022) Flood-related damages constitute a major share of disaster-induced economic losses, accounting for approximately 90% of total natural hazard-related impacts (Chan, 2015). Rapid urban expansion, combined with climate variability and localized high-intensity rainfall, has intensified pressure on conventional drainage systems.

Traditionally, urban stormwater management relied on rapid conveyance approaches, often described as “drain and dispose”, where runoff is efficiently transported through gutters, channels, and pipe networks to receiving water bodies(Butler & Davies, 2010). Although effective in reducing localized ponding, such systems may transfer flood risk downstream and amplify hydrological peaks, while also degrading environmental quality through concentrated pollutant loads (Fletcher et al., 2015) . In response, Sustainable Urban Drainage Systems (SuDS) were introduced to promote runoff attenuation, infiltration, and source control, aiming to replicate natural hydrological processes within urban environments.

Among stormwater control strategies, subsurface drainage systems are widely implemented to manage excess groundwater and surface infiltration. These systems typically consist of buried perforated pipes or modular configurations designed to intercept and convey subsurface flow, reduce waterlogging, stabilize soil conditions, and enhance structural ground performance (Yunianta et al., 2020); (Abdullah et al., 2023). While their performance under steady discharge conditions has been extensively documented, limited research has addressed their hydraulic behaviour under downstream backflow conditions, particularly during flash flood-induced water level surges.

During flash flood events, rapid downstream water level rise may generate backwater effects and partial outlet restriction, thereby modifying velocity distribution, flow depth, and turbulence characteristics within subsurface drainage systems. Such boundary-controlled conditions may significantly alter effective hydraulic resistance and challenge traditional steady-flow design assumptions. Despite its practical importance in flood-resilient design, the interaction between Manning’s roughness coefficient and flow regime under backflow influence remains insufficiently understood.

Therefore, this study experimentally investigates the hydraulic resistance behaviour of subsurface drainage systems subjected to controlled backflow conditions, with particular emphasis on the relationship between roughness, velocity, flow depth, and Froude number across varying longitudinal slopes. By quantifying slope-dependent resistance variability under restricted outflow scenarios, this research aims to provide improved understanding for resilient urban stormwater drainage design.

2. Methodology

2.1 Experimental Setup

The experimental investigation was conducted at the Physical Laboratory of the River Engineering and Urban Drainage Research Centre (REDAC), Universiti Sains Malaysia. Two subsurface drainage configurations were evaluated: a perforated subsurface drain (PSD) and a subsurface drain module (SDM).

The perforated drain tested was a high-density polyethylene (HDPE) sand slot pipe manufactured by Timewell Drainage Products (Timewell, IL, USA). A 3.0 m long testing pipe with an internal diameter of 300 mm was installed in the flume. The pipe consisted of non-staggered internal slots and external perforations designed to facilitate subsurface inflow. Photographic documentation of the sectional and plan views, as well as internal and external slot configurations, is presented in Figure 1.

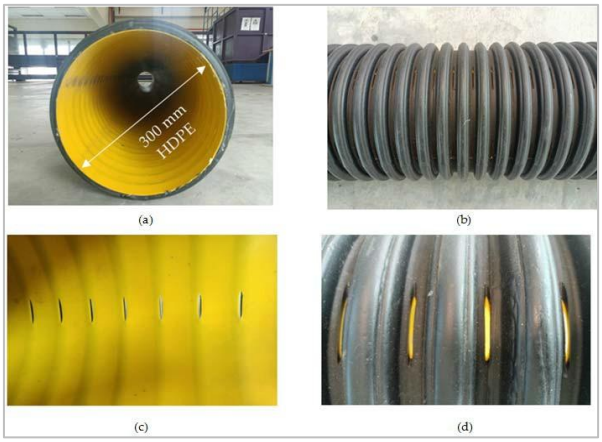

Fig. 1- Photographs of (a) the sectional view and (b) the plan view of the HDPE perforated pipe, as well as views of (c) the non-staggered inner and (d) the outer slots of the perforated pipe used in this work.

The modular configuration consisted of a half-tank subsurface drainage module (200 mm × 220 mm × 710 mm; wall thickness 17.5 mm) supplied by Rainsmart Solutions. The module represents a typical void-based subsurface drainage system used for attenuation and conveyance. A schematic and three-dimensional view are shown in Figure 2.

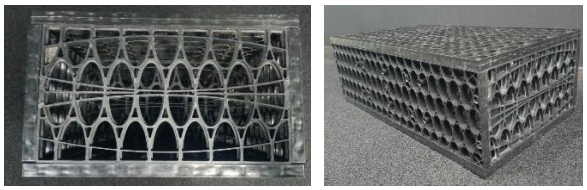

(a) **(b)**

Fig. 2- Module Drain by Rainsmart Solutions. (a) Side View (b) 3D View

Experiments were performed in a 5.9 m long rectangular flume (Figure 3) constructed of reinforced acrylic panels to enable visual flow observation. The flume was equipped with a constant-head inlet tank to ensure uniform inflow distribution and an adjustable downstream gate to simulate controlled outlet restriction. Longitudinal slopes of 1:500, 1:750, and 1:1000 were established using a mechanical jack system, representing typical urban subsurface drainage gradients (Figure 4). Figure 5 shows Perforated Subsurface Drain in Rectangular Flume and Figure 6 shows Top View of Subsurface Drain Module in Rectangular Flume.



Fig. 3- Rectangular Flume at Physical Laboratory, REDAC USM



Fig. 4- The Longitudinal Slope Set Up



Fig. 5- Perforated Subsurface Drain in Rectangular Flume



Fig. 6- Top View of Subsurface Drain Module in Rectangular Flume

To simulate downstream backflow conditions associated with flash flood scenarios, the outlet gate was configured under Gate Partially Open (GPO) condition at a controlled 10 cm water level (Figure 7). This setup allowed evaluation of hydraulic behavior under restricted outflow and induced backwater effects.



Fig. 7- Outlet Condition of Gate Partially Open

2.2 Determination of Flow

Flow characteristics were evaluated through systematic depth and velocity measurements at nine points along the flume, from upstream to downstream. Figure 8 shows the schematic view of the experiment test point. Flow depth (y) was measured using a vertically mounted graduated scale attached to the flume wall. Initial baseline readings were recorded prior to each run to ensure consistency in reference levels. Figure 9 shows the depth measurement of perforated subsurface drain in rectangular flume and Figure 10 shows the determination of flow depth of subsurface drain module (outlet). Velocity measurements were obtained using a Marsh-McBirney Model 2000 Flo-Mate electromagnetic flowmeter (Figure 11), capable of providing real-time velocity readings in meters per second. The device was calibrated before each experimental run, and velocity measurements were recorded to two decimal places. Zero-flow calibration was conducted by submerging the probe in still water to eliminate background noise and ensure accurate low-velocity detection. Measured velocities (Figure 12 & Figure 13) were cross-checked against theoretical discharge estimates derived from hydraulic calculations to verify instrument consistency.

Velocity sampling followed standard hydraulic measurement protocols. For flow depths less than 0.25 m, velocity was measured at 0.6y. For depths equal to or greater than 0.25 m, velocities were measured at 0.2y and 0.8y, and the average value was adopted as the representative section velocity.

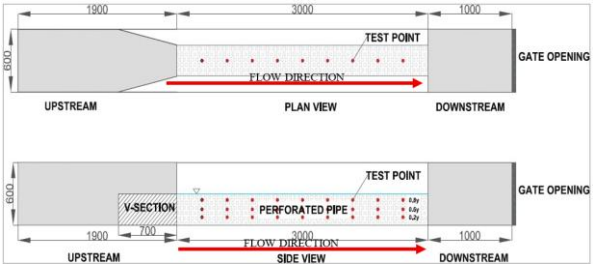

Fig. 8- Schematic View of The Experiment Test Point (unit in mm)



Fig. 9- Depth Measurement of Perforated Subsurface Drain in Rectangular Flume



Fig. 10- Determination of flow depth of subsurface Drain Module (Outlet)



Fig. 11- The Marsh-McBirney Model 2000 Flo-Mate

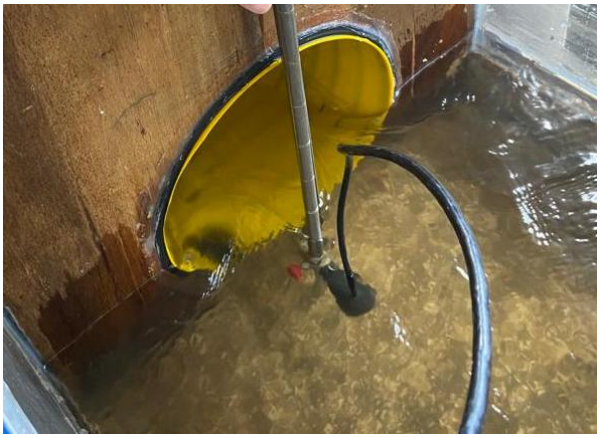

Fig. 12- Velocity Measurement of Flow in Perforated Subsurface Drain



Fig. 13- Velocity Measurement of Flow in Subsurface Drain Module

2.3 Hydraulic Parameter Determination

The hydraulic parameters considered in this study are Froude Number (*Fr*), Reynolds Number (Re), flow depth (*y*), flow velocity, discharge (*Q*) and infiltration time. The analysis of the laboratory results was based on the Manning Formula and was calculated from:

$$n = \frac{1}{v} R^{\frac{2}{3}} S^{\frac{1}{2}} \quad (1)$$

where n = Mannings, v = Velocity (m/s), R = Hydraulic Radius and S = Slope. Froude number relates to the state of flow.

$$Fr = \frac{V}{\sqrt{gD}} \quad (2)$$

where V = Water velocity, D = Hydraulic depth (cross sectional area of flow / top width), g = Gravity Acceleration when $Fr = 1$ (critical flow), $Fr > 1$ (supercritical flow), $Fr < 1$ (subcritical flow). The Reynolds number is defined as the ratio of inertial and viscous forces and can be stated mathematically as:

$$\mathrm{Re} = \frac{Vl}{v} \quad (3)$$

where V = The water velocity, l= Length and v = Kinematic viscosity of the water.

3. Results and Discussion

Figure 14 presents the relationship between Manning's roughness coefficient (n) and flow velocity (v) for both perforated subsurface drain (PSD) and subsurface drain module (SDM) under the Gate Partially Open under controlled backflow conditions with a partially opened gate and a water depth of 10 cm across slopes of 1:500, 1:750, and 1:1000. An inverse relationship between n and v is consistently observed, aligning with Manning's equation, where increased velocity corresponds to reduced hydraulic resistance. Strong linear correlations are recorded at the steeper slope (1:500, $R^2 \approx 0.957$), indicating stable flow behaviour despite partial outlet restriction. However, as the slope decreases, correlation strength reduces (1:750, $R^2 \approx 0.827$) and becomes notably weak at 1:1000 (PSD $R^2 \approx 0.149$; SDM $R^2 \approx 0.332$), reflecting increasing hydraulic instability under downstream backwater influence. The 10 cm gate opening induces a backflow condition that elevates flow depth and disrupts velocity gradients, with PSD showing greater sensitivity due to perforation-induced turbulence, whereas SDM exhibits comparatively more stable flow transitions. These findings indicate that under flash flood-related backflow scenarios, hydraulic resistance becomes increasingly governed by downstream boundary control, particularly at milder gradients.

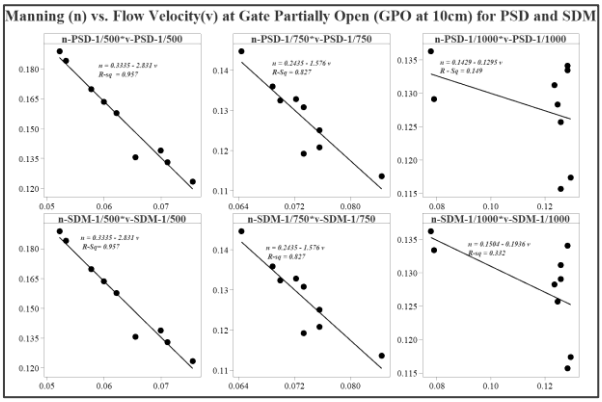

Fig 14- Relationship between manning, *n* and flow Velocity, *v* and under the phases of GPO AT 10cm for PSD and SDM with longitudinal slopes of 1:500, 1:750 and 1:1000.

Figure 15 illustrates the relationship between Manning's roughness coefficient (n) and flow depth (y) for both perforated subsurface drains (PSD) and subsurface drain modules (SDM) under Gate Partially Open under controlled backflow conditions with a partially opened gate and a water depth of 10 cm across slopes of 1:500, 1:750, and 1:1000. Compared to the fully open condition, greater data scattering is observed due to downstream backwater effects, which modify flow depth and increase hydraulic variability. At steeper slopes (1:500 and 1:750), weak linear correlations are recorded for both systems, particularly for PSD, indicating that the interaction between flow depth and hydraulic resistance under partial outflow restriction is not adequately represented by simple linear behavior. This variability reflects unstable flow energy distribution and localized turbulence within the drainage arrangements under partially submerged conditions. At the mildest slope (1:1000), an inverse trend between n and y becomes more apparent, suggesting increasing dominance of backwater-controlled flow behavior. Although the statistical relationships remain relatively weak, the results provide meaningful insight into roughness variation under flash flood-induced backflow scenarios and serve as a preliminary reference for future refinement of predictive subsurface drainage models.

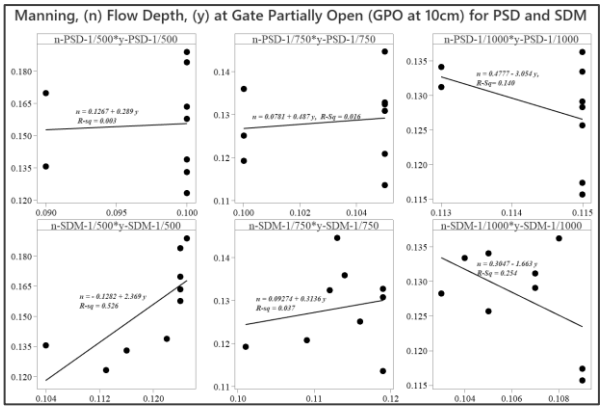

Fig 15- Relationship between Manning, n and Flow depth, y and under the phases of GPO AT 10cm for PSD and SDM with longitudinal slopes of 1:500, 1:750 and 1:1000.

Figure 16 presents the relationship between Manning's roughness coefficient (n) and Froude number (Fr) under Gate Partially Open (10 cm) conditions for both PSD and SDM systems across slopes of 1:500, 1:750, and 1:1000. At the steeper slope (1:500), PSD demonstrates a noticeable reduction in n with increasing Fr, indicating decreasing hydraulic resistance as flow transitions toward higher inertial dominance, whereas SDM exhibits a comparatively more moderate reduction, suggesting increased flow stability within the modular configuration. At 1:750 slope, PSD shows greater variability in n around transitional Fr values, reflecting sensitivity to backwater-induced disturbances, while SDM maintains relatively consistent roughness behaviour. At the mildest slope (1:1000), both systems display altered n–Fr trends under restricted outflow, indicating increasing influence of downstream backwater control over internal flow dynamics. Notably, SDM consistently records slightly higher n values at mild slopes, implying enhanced internal energy dissipation under partially submerged conditions. Overall, the results demonstrate that under flash flood-associated backflow, the interaction between flow regime and hydraulic resistance becomes increasingly slope-dependent, with modular systems exhibiting comparatively more stable resistance characteristics.

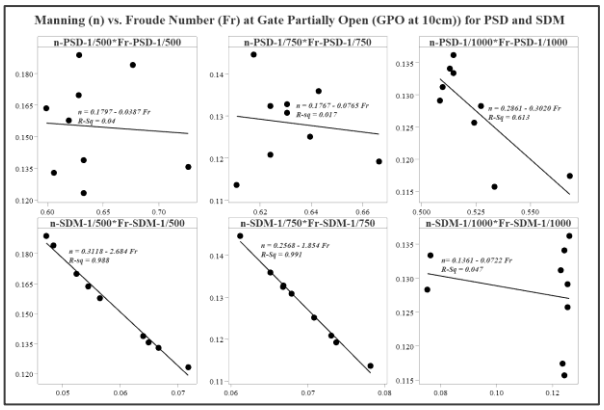

Fig 16- Relationship between Manning, n and Froude Number, Fr and under the phases of GPO AT 10cm for PSD and SDM with longitudinal slopes of 1:500, 1:750 and 1:1000.

4. Conclusion

This study experimentally evaluated the hydraulic resistance behaviour of perforated subsurface drains (PSD) and subsurface drain modules (SDM) under downstream backflow conditions simulated by a partially open gate (10 cm). Across longitudinal bed slopes, an inverse relationship between Manning's roughness coefficient (n) and velocity (v) was consistently observed, confirming that hydraulic resistance decreases with increasing inertial dominance. However, the stability of this relationship was slope-dependent, with strong correlations at 1:500 and significant deterioration at 1:1000, indicating increasing influence of downstream boundary control under mild gradients.

The relationship between n and flow depth (y) exhibited weak linearity, particularly under partially submerged conditions, suggesting that effective roughness under backflow cannot be solely described by depth variation. Instead, localized turbulence and fluctuating energy gradients dominate resistance behaviour in restricted outlet scenarios.

Similarly, the relationship between n and Fr indicates that flow regime transition significantly influences resistance behavior in resistance modulation. At steeper slopes, n decreased with increasing Fr, while at milder slopes, altered trends were observed, indicating a shift from slope-controlled to backwater-controlled hydraulic response. SDM demonstrated comparatively more stable resistance behaviour than PSD under fluctuating backflow conditions, suggesting improved adaptability of modular configurations in transient stormwater systems.

Overall, the findings demonstrate that under flood-associated backflow, hydraulic resistance in subsurface drains becomes strongly governed by downstream boundary conditions and longitudinal slope. These results highlight the importance of considering backflow-induced roughness variability in the design and modelling of urban subsurface stormwater drainage systems.

Acknowledgement

The authors express their gratitude to Ministry of Higher Education, Malaysia, under the Higher Institution Centre of Excellence (HICoE) for a research grant under HICoE Niche area Sustainable Urban Stormwater Management (Grant No. A305-LR-AKH001-0004403901-0000) and Short-Term Research Grant- Q (R501-LR-RND002-0000001279-0000) Universiti Sains Malaysia for providing the funding and the facilities.

References

[1] Abdullah, J., Mohd Arif Zainol, M. R. R., Riahi, A., Zakaria, N. A., Yusof, M. F., Shaharuddin, S., Alias, M. N., Mohd Kasim, M. Z., Abdul Aziz, M. S., Mohamed Noor, N., Zawawi, M. H., & Ikhsan, J. (2023). Investigating the Relationship between the Manning Coefficients (n) of a Perforated Subsurface Stormwater Drainage Pipe and the Hydraulic Parameters. *Sustainability*, *15*(8). https://doi.org/10.3390/su15086929

[2] Chan, N. W. (2015). Impacts of Disasters and Disaster Risk Management in Malaysia: The Case of Floods. In D. P. Aldrich, S. Oum, & Y. Sawada (Eds.), *Resilience and Recovery in Asian Disasters: Community Ties, Market*

Mechanisms, and Governance (pp. 239–265). Springer Japan. https://doi.org/10.1007/978-4-431-55022-8_12

[3] Butler, & John Davies. (2010). *Urban Drainage: ISBN: 041545526X* (3rd ed.). Taylor & Francis.

[4] Fletcher, T. D., Shuster, W., Hunt, W. F., Ashley, R., Butler, D., Arthur, S., Trowsdale, S., Barraud, S., Semadeni-Davies, A., Bertrand-Krajewski, J.-L., Mikkelsen, P. S., Rivard, G., Uhl, M., Dagenais, D., & Viklander, M. (2015). SUDS, LID, BMPs, WSUD and more – The evolution and application of terminology surrounding urban drainage. *Urban Water Journal*, *12*(7), 525–542. https://doi.org/10.1080/1573062X.2014.916314

[5] Hammond, M. J., Chen, A. S., Djordjević, S., Butler, D., & Mark, O. (2015). Urban flood impact assessment: A state-of-the-art review. *Urban Water Journal*, *12*(1), 14–29. https://doi.org/10.1080/1573062X.2013.857421

[6] Maqtan, R., Othman, F., Jaafar, W., Sherif, M., & El-Shafie, A. (2022). A scoping review of flash floods in Malaysia: current status and the way forward. *Natural Hazards*, *114*, 1–30. https://doi.org/10.1007/s11069-022-05486-6

[7] Milica Dordevic, Petra Mutic, & Hwirin Kim. (2020, March 23). *Flash Flood Guidance System: Response to one of the deadliest hazards*.

[8] Si, Y., Li, J., & Si, Y. (2023). Urban Flood Loss Estimation and Evacuation Design Based on a 500-Year Extreme Flood Event in Syracuse City. *Water*, *15*(1). https://doi.org/10.3390/w15010003

[9] Yunianta, A., Suripin, S., & Setiadji, B. (2020). Application of Sustainable Road Drainage System: Simulation by Using SWMM Program. *Civil Engineering and Architecture*, *8*, 55–65. https://doi.org/10.13189/cea.2020.080203